Investigations of Osmium Deposits on a Pt(111) Electrode in Relation to Heterogeneous Electrocatalysis

A. Wieckowski,[1] H. You,[2] C.K. Rhee,[1] Y. Tolmachev,[2] K. Attenkofer,[2] M. Wakisaka[1]
[1]Department of Chemistry, University of Illinois at Urbana-Champaign (UIUC), Urbana, IL, U.S.A.
[2]Materials Science Division, Argonne National Laboratory, Argonne, IL, U.S.A.

Introduction

One obstacle to overcome in order to make direct methanol fuel cells (DMFCs) practical is the lack of efficient, poison-tolerant anode catalysts [1]. In the oxidation of methanol on platinum, surface CO is formed as a stable product. It blocks catalytic sites and inhibits further methanol oxidation. A good anode catalyst for DMFCs must transform the poisonous CO to CO_2 by using the oxygen atoms available in the interfacial water or in water decomposition products like adsorbed OH species. The release of surface sites from CO would allow for catalytic, relatively high-turnover methanol oxidation. Toward this end, Pt surfaces have been modified with various admetals to change the CO-surface-binding properties and lessen the effect of CO poisoning [2].

The most active methanol oxidation catalysts are Pt-based ternaries or even quaternaries that contain osmium (Os) as one of the catalyst components (e.g., Pt/Ru/Os and Pt/Ru/Os/Ir [3, 4]). The role of Os surface structure and oxidation states in methanol oxidation electrocatalysis, however, remains unclear and merits further study. We have therefore investigated the Os island chemical state on Pt(111) by *in situ* grazing incidence fluorescence x-ray absorption spectroscopy (GIF-XAS). Other relevant data were obtained by ultrahigh vacuum (UHV) x-ray photoemission spectroscopy (XPS) of Pt(111)/Os and by *in situ* scanning tunneling microscopy (STM). Oxidation states of Os spontaneously deposited on Pt(111) are revealed in conjunction with the results of previous measurements of methanol oxidation activity on the nanostructured Pt(111)/Os surfaces [5].

Methods and Materials

A platinum single crystal of Pt(111) orientation (10 mm in diameter, <0.5°, Accumet Materials) was used for all characterization experiments. For GIF-XAS, the Pt(111) crystal was annealed in a hydrogen flame, cooled for 1 minute in an Ar/H_2 gas mixture, and then dipped into high-purity water to protect the surface from contamination. The water-protected Pt(111) was transferred into a reflection-type cell covered with a Kapton® (8-μm-thick) window. The electrode was then exposed to 1 mM $OsCl_3$ (hydrated $OsCl_3$, Premion®, 99.99%, Alfa Aesar) + 0.1 M H_2SO_4 solution for 5 minutes, with no external potential applied. After exposure to the Os solution, the electrode was rinsed with 0.1 M H_2SO_4, and the electrode potential was cycled from 100 to 800 mV versus the reversible hydrogen electrode (RHE) at 50 mV/s in 0.1 M H_2SO_4 until a steady-state voltammogram was observed (about nine times). This method of Os deposition is called "spontaneous deposition." Ref. 6 has details on electrochemical, electrochemical-STM (EC-STM) and XPS results, mentioned here only briefly.

The GIF-XAS experiments were performed by using a thin-layer film cell, in which the path length was on the order of tens of microns. A Si(220) double-crystal monochromator was used for beam energy selection. A Pd-coated toroidal mirror was used to focus the beam of linearly polarized x-rays to ~0.5 mm^2. Another Pd-coated mirror was used to further reject higher harmonics. The crystal surface was aligned to be nearly horizontal (s-polarization), making a 0.55° grazing angle with the incoming x-ray beam. The energy window of the detector electronics was narrowly set around Os L_α fluorescence (~8.9 keV), but no filters were employed. The major contribution to the background signal was Pt L_α fluorescence (9.44 keV) excited by the second harmonic contamination in the beam, which is too close in energy to the Os L_α to be completely filtered with the Ge detector.

Results

EC-STM and XPS Measurements of Pt(111)/Os

After spontaneous deposition of Os on Pt(111), EC-STM reveals that nanoislands of Os are formed. They are 2-5 nm wide and 0.27-0.32 nm high; this height is close to the expected height of one Os atom (about 0.22-0.27 nm). The surface area coverage of Os was found to be 75 ±15%. XPS results were obtained after holding the Pt(111)/Os electrode at the specified potential for 1 minute (Fig. 1), emersing the electrode into argon atmosphere, and then transferring it to UHV without exposure to air [6]. For emersion potentials below 500 mV, only one Os $4f_{7/2}$ peak appears at 50.8 eV; it is attributable to Os(0). Starting at 600 mV, the Os(0) deposit is oxidized partially to Os(IV), shown by peaks at 51.5 eV. At 900 mV, the $4f_{7/2}$ peak appears at 51.1 eV, between those of Os(IV) and Os(0). A similar Os species was observed by other investigators, and the formal valency was estimated to be +1.6 [7]. Emersion

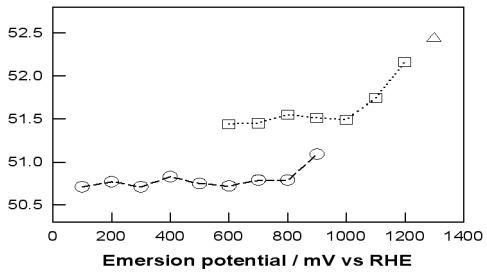

FIG 1. The variation of the binding energy of the Os ***4f****$_{7/2}$ peak of spontaneously deposited Os layers on the Pt(111) electrode. Circles, squares, and triangles correspond to Os(0), Os(IV), and Os(VIII) species, respectively.*

at 1100 and 1200 mV shows the $4f_{7/2}$ peak shifted to higher values, but not high enough for it to be assigned to Os(VIII) on the basis of the Pourbaix diagram. At 1300 mV, however, assignment of the binding energy to Os(VIII) is possible (52.4 ±0.1 eV). Evidently, the oxidation state of Os at 1100–1200 mV is between Os(IV) and Os(VIII). Additionally, the amount of Os on the surface at each emersion potential was determined by comparing the area of the Os $4f_{7/2}$ peaks to the Pt $5p_{3/2}$ peaks [6]. The amount of Os on the surface decreases starting at 1000 mV, and Os is no longer detectable at 1400 mV. The dissolution of Os at these potentials has been confirmed by cyclic voltammetry [6].

GIF-XAS measurement of Pt(111)/Os

Figure 2 shows GIF-XAS spectra of Os spontaneously deposited on Pt(111) at four different electrode potentials (300, 500, 900, and 1100 mV). The edge jump heights were fit and normalized to unity to compensate for the loss of Os at high electrode potentials so that the spectra could be compared to determine chemical changes of Os. As the electrode potential moved in the anodic (oxidizing) direction, the white line in the Os x-ray absorption spectrum (i.e., the x-ray energy at the maximum absorption) increased in height, and the absorption edge shifted toward higher

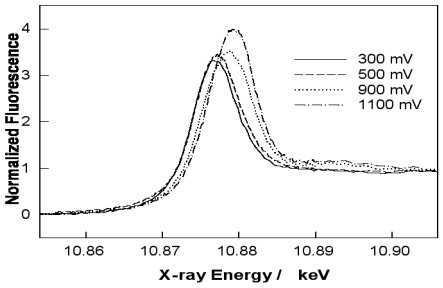

FIG 2. Normalized fluorescence L_{III}-edge GIF-XAS spectra of Os spontaneously deposited on Pt(111) at 300, 500, 900, and 1100 mV.

energies. These observations strongly indicate, following the Fermi golden rule, a decrease in the electronic occupancy of the 5d states, mainly due to the oxidation of Os.

Summarized in Fig. 3(a) are the changes in the x-ray energies of the white lines and the rising and falling edges of the white lines as a function of electrode potential. Three electrode potential regions are distinguishable: (1) from 100 to 500 mV, with constant GIF-XAS parameters; (2) between 500 and 1000 mV, with a gradual shift in the edge and peak positions; and (3) between 1.1 and 1.4 V, characterized by limiting values. Because these parameters are related to the oxidation states of Os sampled by the x-ray, Fig. 3(a) as obtained with the *in situ* GIF-XAS is equivalent to the results of the *ex situ* XPS (Fig. 1). In the first region, constant parameters indicate metallic Os, which is in agreement with XPS results. The observed white line intensity (NF = 3.35), however, is larger than that reported for metallic bulk Os (NF = 2.0) [8]. This may result from the difference in the electronic properties of the metallic Os layers on Pt(111) and the metallic bulk Os. The 5d electrons in Os and Pt may form a mixed electronic band, and the densities of electronic states near the Fermi level may not be the same as they are in metallic bulk Os.

Between 500 and 1000 mV, the white-line intensity increases, and the peaks broaden (up to 8.2 eV versus 6.7 eV), which includes a gradual shift in edge and peak positions. These changes can be explained by the presence of two different Os species on Pt(111), as revealed by XPS. Between 1.0 and 1.40 V, the rising edge and peak positions reach the limiting values of 10.8753 keV at NF = 2 and 10.8793 keV, respectively. Also, the white-line intensity increases to 4 NF units. Flushing of the Kapton film thin layer with the background electrolyte (refer to the two points at 1200 mV) reduced the amount of Os sampled by x-rays without appreciably changing the GIF-XAS parameters. These data suggest that the Os species has a higher oxidation state and that it is partially soluble, while the rest remains on the surface. In fact, OsO_4 ideally fits this profile, and it also fits the data at 1.3 V in the *ex situ* XPS study (Fig. 1).

Discussion

The results from EC-STM, *ex situ* XPS, and *in situ* GIF-XAS offer a fairly detailed picture of Pt(111)/Os. According to XPS, the adsorbed Os layer is metallic below 600 mV, and there is no binding energy shift between the bulk Os and the deposited Os. In contrast, the GIF-XAS results suggest a significant electron transfer from Os to Pt in this potential region. This discrepancy between XPS and GIF-XAS measurements should be investigated in the future.

Here we now attempt to relate the oxidation states of

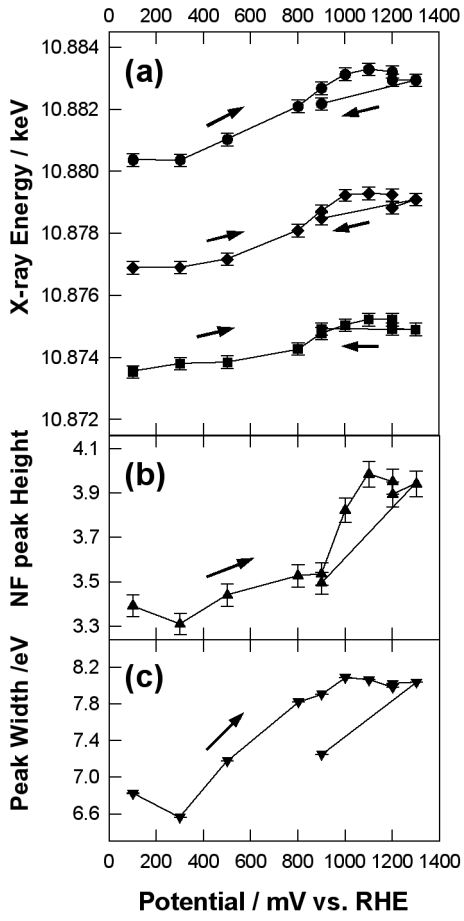

FIG 3. GIF-XAS parameters as functions of the electrode potential. (a) The energies of the white-line peak (closed diamonds, middle line) and its rising (closed squares, bottom line) and falling (closed circles, top line) sides at NF = 2. (b) The normalized fluorescence white-line peak height at NF = 2. (c) The normalized fluorescence white-line peak width at NF = 2.

Os to the electrocatalytic activity of nanostructured Pt(111)/Os electrodes toward methanol oxidation, as previously measured by using chronoamperometry [5]. The presence of an Os deposit on Pt(111) enhanced the current density of methanol oxidation by a factor of 25 (i.e., from 0.4 $\mu A \cdot cm^{-2}$ without Os to 10 $\mu A \cdot cm^{-2}$ with Os at 400 mV, a potential where only a metallic Os layer exists). Clearly, the metallic state of Os played a significant role in the catalytic enhancement of Pt by Os. According to the bifunctional mechanism [1], the role of the metallic Os is to activate water as a source of oxygen for the oxidation of methanol. When half of the osmium is in the Os(IV) state (i.e., at 700 mV), the methanol oxidation current density of Pt(111)/Os increases to 230 $\mu A \cdot cm^{-2}$, demonstrating the activity of OsO_2 as well (as at least not suppressing the oxidation rate). These issues will be examined further since they are not yet sufficiently understood.

One could compare the results on Os oxidation states studied in this report with results on ruthenium (Ru) oxide formation on Pt(111) [9]. The potential of Ru oxide formation (400 mV) on platinum is definitely lower than that of Os (600 mV), which suggests that in terms of the catalytic electrooxidation properties, Ru is more oxophilic than Os on Pt(111). The difference in the oxophilicity of Ru and Os on Pt(111) may account for the difference in methanol oxidation activity at low potentials [5]. This difference, however, either disappears or is much less favorable for Ru at higher potentials than about 500 mV [5].

Acknowledgments

Use of the APS was supported by the U.S. Department of Energy (DOE), Office of Science, Office of Basic Energy Sciences, under Contract No. W-31-109-ENG-38. This work was also supported by the DOE Division of Materials Sciences under Award No. DEFG02-91ER45439, through the Frederick Seitz Materials Research Laboratory at UIUC. This report is excerpted from Ref. 6.

References

[1] A. Hamnett, in *Interfacial Electrochemistry: Experimental, Theory and Applications*, edited by A. Wieckowski (Marcel Dekker, New York, NY, 1999), p. 843.

[2] P.N. Ross, Jr., in *Electrocatalysis*, *Frontiers of Electrochemistry*, edited by J. Lipkowski and P.N. Ross, Jr. (Wiley-VCH Publishers, New York, NY, 1998), Vol. 4, p. 43.

[3] B. Gurau et al., J. Phys. Chem. B **102**, 9997 (1998).

[4] E. Reddington, A. Sapienza, B. Gurau, R. Viswanathan, S. Sarangapani, E.S. Smotkin, and T.E. Mallouk, Science **280**, 1735 (1998).

[5] A. Crown, I.R. Moraes, and A. Wieckowski, J. Electroanal. Chem. **500**, 333 (2001).

[6] C.K. Rhee, M. Wakisaka, Y. Tolmachev, C. Johnston, R. Haasch, K. Attenkofer, G.-Q. Lu, H. You, and A. Wieckowski, J. Electroanal. Chem. **554-555**, 367 (2003).

[7] Y. Hayakawa, K. Fukuzaki, S. Kohiki, Y. Shibata, T. Matsuo, K. Wagatsuma, and M. Oku, Thin Solid Films **347**, 56 (1999).

[8] G. Meitzner, G.H. Via, F.W. Lytle, and J.H. Sinfelt, J. Phys. Chem. **96**, 4960 (1992).

[9] H. Kim, I.R. de Moraes, G. Tremiliosi, R. Haasch, and A. Wieckowski, Surf. Sci. **474**, L203 (2001).